**Cell Metabolism, Volume *35***

## Supplemental information

# Immunoediting instructs tumor metabolic reprogramming to support immune evasion

**Chin-Hsien Tsai, Yu-Ming Chuang, Xiaoyun Li, Yi-Ru Yu, Sheue-Fen Tzeng, Shao Thing Teoh, Katherine E. Lindblad, Mario Di Matteo, Wan-Chen Cheng, Pei-Chun Hsueh, Kung-Chi Kao, Hana Imrichova, Likun Duan, Hector Gallart-Ayala, Pei-Wen Hsiao, Massimiliano Mazzone, Julijana Ivanesevic, Xiaojing Liu, Karin E. de Visser, Amaia Lujambio, Sophia Y. Lunt, Susan M. Kaech, and Ping-Chih Ho**

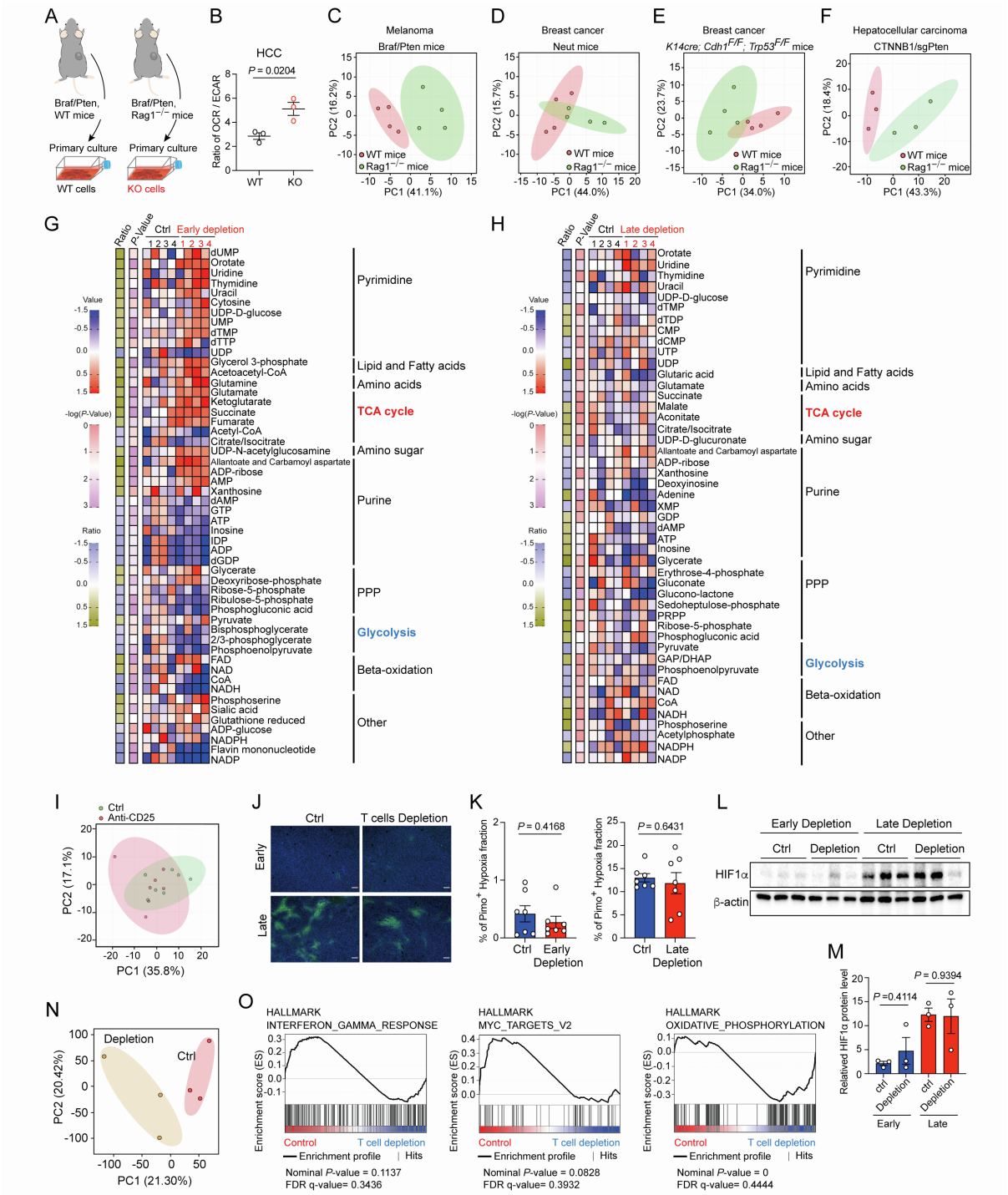


**Figure S1. Immunosurveillance controls metabolic states in tumors in the hypoxia- and HIF1α-independent mechanism, Related to Figure 1.**

(**A**) Experimental scheme for generating primary Braf/Pten melanoma cells from immunocompetent Braf/Pten mice (WT cells) and adaptive immune cell-deficient Braf/Pten mouse (KO cells). (**b**) Basal OCR/EACR in the primary HCC cells harboring β-catenin overexpression and Pten deletion derived from immunocompetent mice (WT cells) or Rag1$^{-/-}$ mice (KO cells). (**C-F**) Principal component analysis (PCA) of metabolites in Braf/Pten melanomas (**C**), Neut breast cancers (**D**), K14-Cre; p53$^{f/f}$; Ecad$^{f/f}$ breast cancers (**E**), and hepatocellular carcinoma driven by β-catenin overexpression and Pten

deletion (**F**) derived from immunocompetent wild type mice (WT mice) or $Rag1^{-/-}$ mice. and early T cell depletion. (**G-H**) Heatmap of metabolite levels in Braf/Pten melanomas from control versus early T cell depletion (**G**) or control versus late T cell depletion (**H)**. (**I**) PCA for significantly differential genes expression of Braf/Pten tumor-bearing with indicated treatment, n=7 per group. (**J-K**) Representative images (**J**) and quantification results (**K**) for pimonidazole staining in tumors with indicated treatments (n=7 per group). (**L-M**) Representative immunoblots of HIF1α and β-actin (**L**) and quantification of relative HIF1α protein expression (**M**) in Braf/Pten melanomas from indicated groups. (**N**) PCA of transcriptome for $GFP^+$ melanoma cells isolated from Braf/Pten-mTmG mice receiving either PBS treatment (control) or anti-CD4/CD8 mAbs (depletion) as illustrated in Figure 1N (n=3 per group). (**O)** Gene set enrichment analysis showing upregulated expression of genes on IFNγ response and cMyc targets, but down-regulated expression of genes on oxidative phosphorylation, in $GFP^+$ melanoma cells isolated from Braf/Pten-mTmG mice receiving PBS treatment compared to Braf/Pten-mTmG mice receiving anti-CD4/CD8 mAbs. Each symbol represents one individual, and data are mean ± s.e.m. and analyzed by unpaired, two-tailed Student's t-test (K and M).

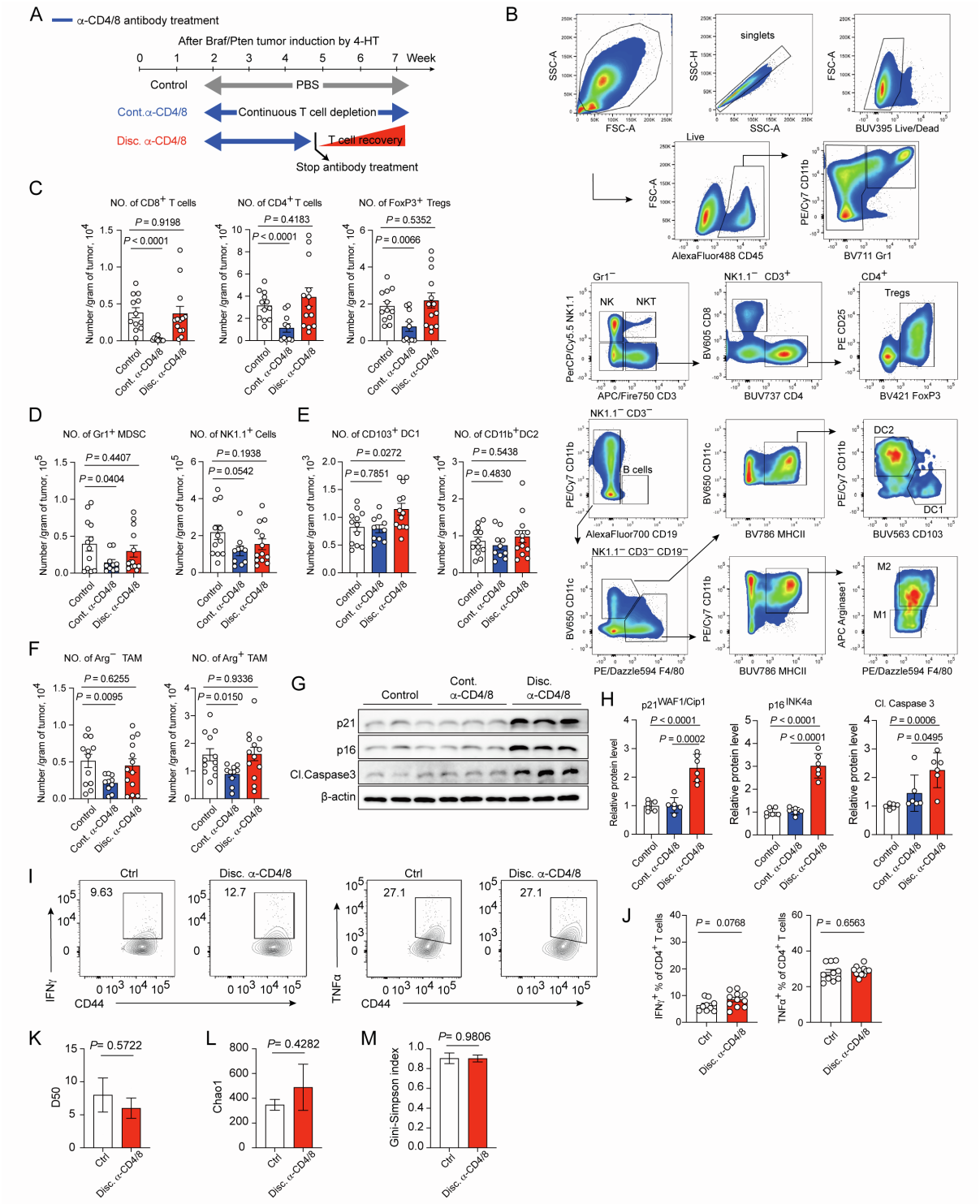


**Figure S2. Re-emergence of T cells restricts growth in non-edited melanomas, Related to Figure 2.**

(**A**) Experimental outline of antibody-based T cell depletion and discontinuation of depletion in murine Braf/Pten melanomas post tumor induction with 4-hydroxytamoxifen (4-HT). (**B**) Gating strategy of flow cytometry analysis for tumor-infiltrating lymphocytes. (**C**) The abundance of T lymphocytes, including $CD8^+$ T cells (left), $CD4^+$ T cells (middle), and $CD4^+$ $FoxP3^+$ Tregs (right) in the indicated tumors. (**D-F**) The abundance of $Gr1^+$ myeloid-derived suppressor cells (MDSCs) (**D**, left panel), NK

cells (**D**, right panel), $CD103^+$ type I conventional dendritic cells ($CD103^+$ DC1) (**E**, left), $CD11b^+$ type I conventional dendritic cells ($CD11b^+$ DC2) (**E**, right), and arginase (Arg) positive and negative tumor-associated macrophages (TAM) (**F**). **(G-H)** Representative immunoblots (**G**) and quantitative results (**H**) of indicated proteins in tumor samples from indicated groups. (**I-J**) Representative plots (**I**) and quantitative results (**J**) of IFNγ-producing and TNFα-producing cells among total tumor-infiltrating $CD44^+$ $CD4^+$ T cells from the indicated mice. (**K-M**) Mouse TCR clonality was examined by Amplicon-seq on TCR-β of $CD45^+CD3^+CD8^+CD44^+$ TILs sorted from Braf/Pten melanomas from control and discontinued groups, followed by calculations of the D55 diversity index (**K**), Chao1 diversity (**L**), and Gini-Simpson index (**M**). Data are the cumulative results from at least two independent experiments, and each symbol represents one individual. Data are mean±s.e.m.; unpaired, two-tailed Student's t-test (C-F, H, and J-M).

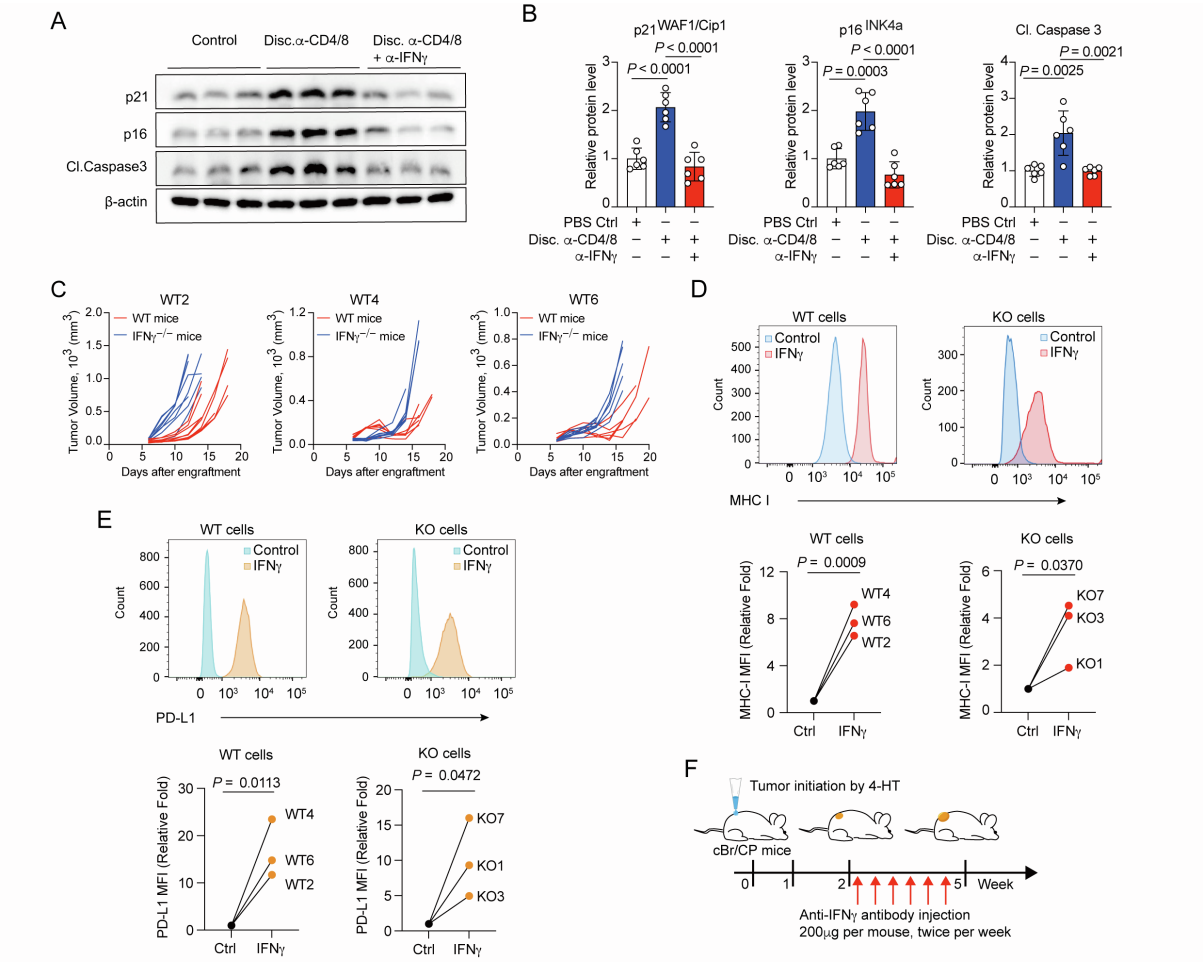


**Figure S3. The re-emergence of T cells restricts growth of melanomas arising in the absence of T cells via IFNγ, Related to Figure 3**

(**A-B**) Representative immunoblot (**A**) and quantitative results (**B**) of indicated proteins in tumor samples from indicated groups. (**C**) Tumor growth curve for WT2, WT4, and WT6, three Braf/Pten melanoma cell lines derived from immunocompetent Braf/Pten mouse, after subcutaneously engrafted into C57BL/6 wild type mice and IFNγ$^{-/-}$ mice (n = 5-8 per group). (**D-E**) Representative histogram showing MHCI (**D**) and PD-L1 (**E**) levels in indicated primary Braf/Pten melanoma cells treated with or without IFNγ (100ng/mL) for 24 hrs. Bottom panels: quantitative results of the geometric mean fluorescence intensity (MFI) of indicated protein from indicated cells. (**F**) Experimental outline of antibody-based early IFNγ neutralization with α-IFNγ antibody in murine Braf/Pten melanomas 2 weeks post tumor induction with 4-hydroxytamoxifen (4-HT). Data are representative or cumulative results of two independent experiments with similar results (A-E). Each symbol represents one individual, and data are analyzed by two-tailed, paired (D-E) or unpaired (B-C) Student's t-test.

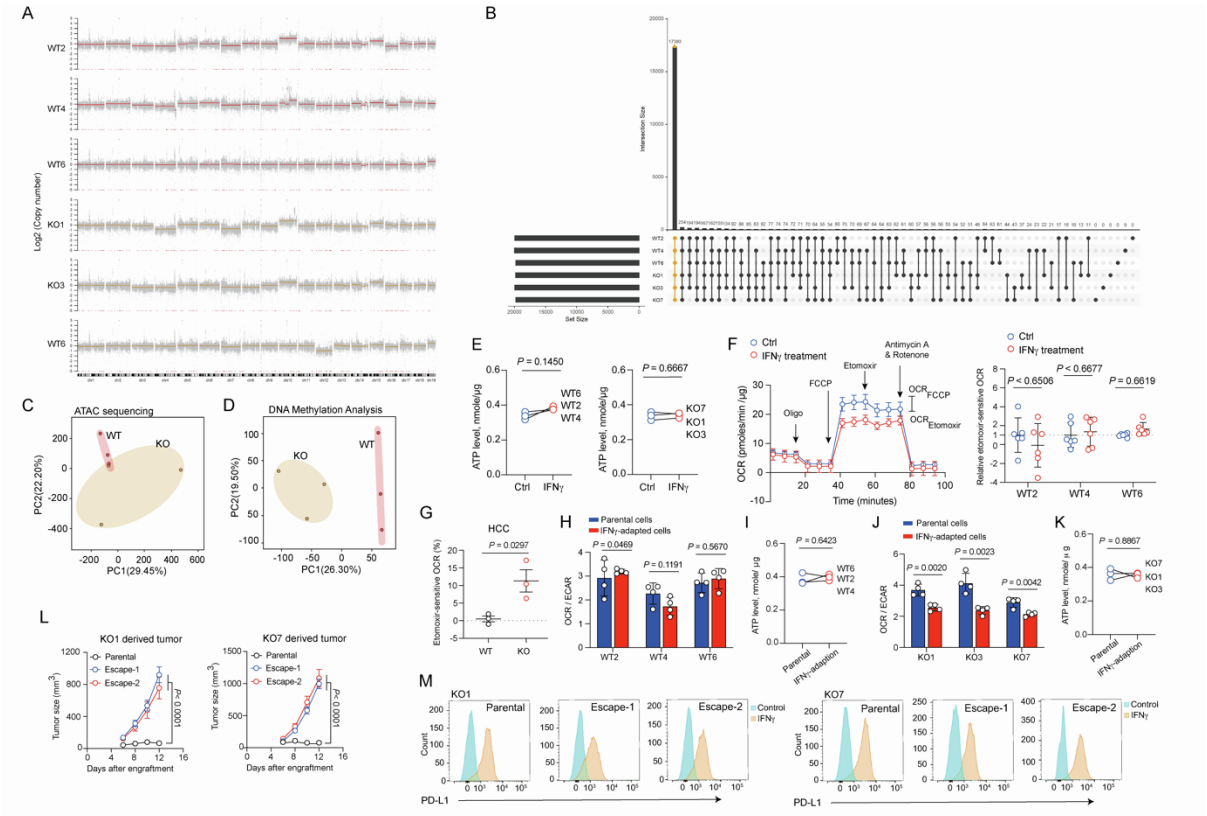

**Figure S4. T cell immunosurveillance modulates metabolic and epigenetic programs in melanoma cells, Related to Figure 4.**

(**A**) Similarity and variation in exome sequencing among indicated primary Braf/Pten melanoma cell lines. (**B**) Single nucleotide variation plots among indicated primary Braf/Pten melanoma cell lines. Bars in the y-axis represent the total number of mutations in each sample. Bars in the x-axis represent the number of mutations shared across samples connected by the black dots in the body of the plot. (**C-D**) PCA of differentially accessible chromatin loci (C) and DNA methylation patterns (D) in primary Braf/Pten melanoma cells derived from immunocompetent Braf/Pten mice (WT cells) and adaptive immune cell-deficient Braf/Pten mouse (KO cells). (**E**) ATP level of WT primary melanoma cells (left) and KO primary melanoma cells (right) treated with or without IFNγ treatment (100ng/mL) for 2 days. (**F**) Representative kinetic of OCR (left panel) following treatment with oligomycin (2 μM), FCCP (2 μM), etomoxir (40 μM) and antimycin A plus Rotenone (0.5 μM each) in WT primary melanoma cells. Cells were incubated with control vehicle (Ctrl) or 100 ng $ml^{-1}$ of IFNγ for 48 hrs prior to assay. Relative etomoxir-sensitive OCR, calculated by measuring the differences of OCR levels between etomoxir and FCCP treatment, in indicated primary melanoma cells treated with control vehicle and IFNγ 48 hours prior to assay (right panel) (n=6 per group). (**G**) Percentage of OCR reduction in response to etomoxir treatment in HCC WT and KO cells (Each symbol represents average value for each treatment, n=5). (**H-I**) Basal OCR/ECAR ratios (**H**) and ATP level (**I**) of parental and IFNγ-adapted WT2, WT4, and WT6 cells. (**J-K**) Basal OCR/ECAR ratio (**J**) and ATP level (**K**) of parental and IFNγ-adapted cells for KO1, KO3, and KO7 cells. (**L**) Tumor growth curve for parental KO1 and escaped KO1 cell lines (left

panel) and parental KO7 and escaped KO7 cell lines (right panel) upon subcutaneously engrafted into immunocompetent C57BL/6 mice (n = 5-8 per group). (**M**) Representative histogram of the geometric MFI for PD-L1 expression in KO1 parental cells and KO1-derived escaped cells (upper) and KO7 parental cells and KO7-derived escaped cells (bottom) in response to control treatment and IFNγ. Data are representative of two independent experiments with similar results. Each symbol represents one individual and data are analyzed by two-tailed, paired (E, I and K) or unpaired (F, G, and L) Student's t-test.

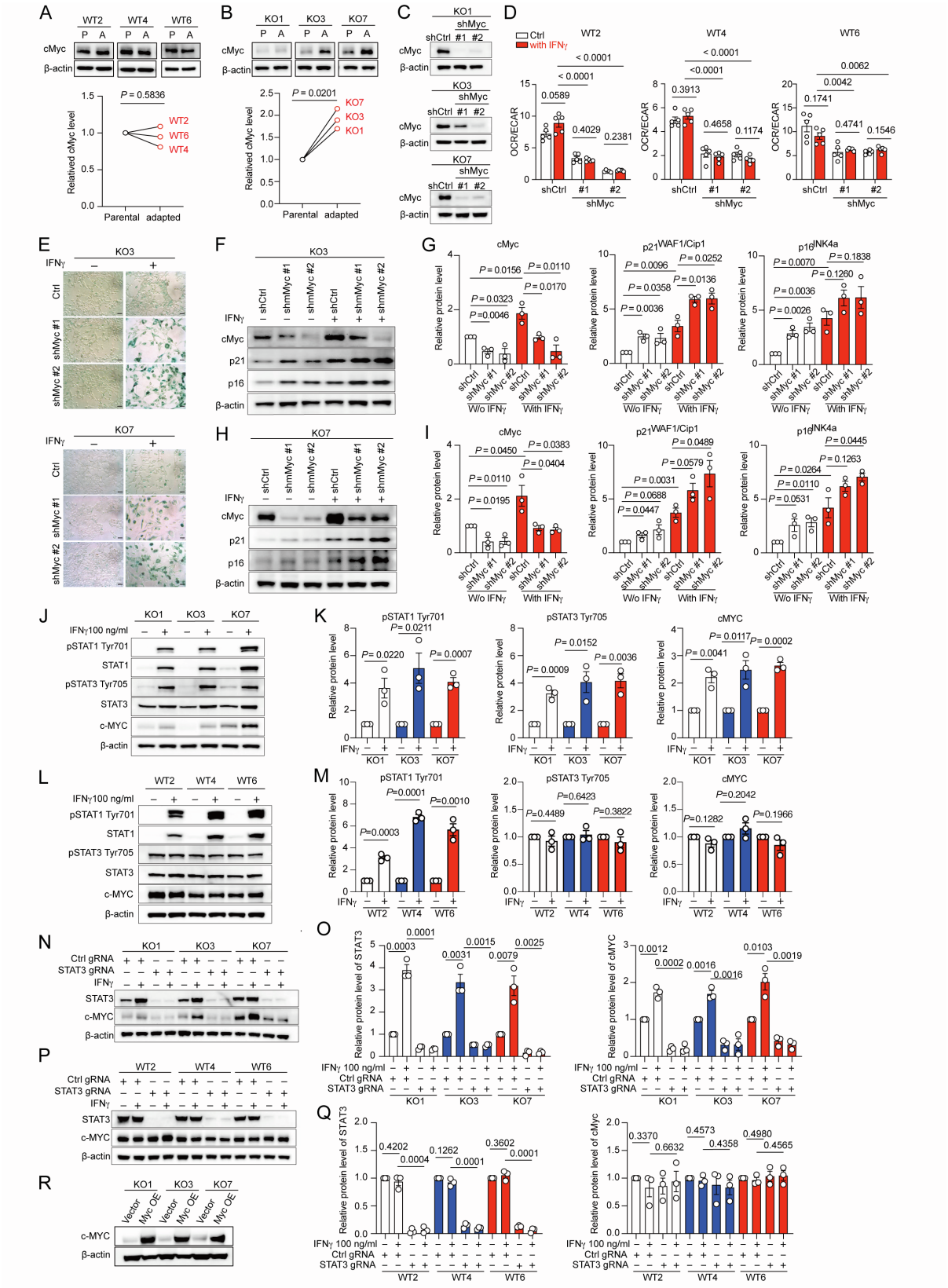

**Figure S5. IFNγ-induced cMyc upregulation suppresses senescence, Related to Figure 5.**

(**A**) Representative immunoblots (upper panel) and quantitative results (bottom panel) of cMyc and β-actin in indicated parental WT Braf/Pten melanoma cells and IFNγ-adapted cells. (*P*, parental cells; *A*, IFNγ-adapted cells). (**B**) Representative immunoblots (upper panel) and quantitative results (bottom

panel) of cMyc and β-actin in indicated parental KO Braf/Pten melanoma cells and IFNγ-adapted cells. (*P*, parental cells; *A*, IFNγ-adapted cells). (**C**) Representative immunoblot of cMyc and β-actin in indicated cells transfected with short hairpin RNAs targeting scramble sequence (shCtrl) or cMyc (shMyc #1, #2). (**D**) Ratios of basal OCR/EACR in indicated WT cells transfected with short hairpin RNAs targeting scramble sequence (shCtrl) or cMyc sequence (shMyc #1 and shMyc #2). Cells were incubated with or without 100 ng $mL^{-1}$ of IFNγ for 48 hours prior to assay. (**E**) Represented staining of β-gal activity in KO3 or KO7 cells transfected with short hairpin RNAs targeting scramble sequence (shCtrl) or cMyc sequence (shMyc #1 and shMyc #2) upon exposure with or without IFNγ for 4 days. (**F-G**) Representative immunoblots (**F**) and quantitative results (**G**) of indicated proteins in KO3 cells expressing control short hairpin RNA (shCtrl) or cMyc short hairpin RNAs (shMyc #1, #2) upon exposure with or without IFNγ for 16 hours. (**H-I**) Representative immunoblots (**H**) and quantitative results (**I**) of indicated proteins in KO7 cells expressing control short hairpin RNA (shCtrl) or cMyc short hairpin RNAs (shMyc #1, #2) upon exposure with or without IFNγ for 16 hours. (**J-K**) Representative immunoblots (**J**) and quantitative results (**K**) of indicated proteins in KO cells with indicated treatment. (**L-M**) Representative immunoblots (**L**) and quantitative results (**M**) of indicated proteins in WT cells with indicated treatment. (**N-O**) Representative immunoblots (**N**) and quantitative results (**O**) of indicated proteins in KO cells expressing control gRNA (Ctrl gRNA) or gRNAs targeting STAT3 (STAT3 gRNA) upon exposure with or without IFNγ for 16 hours. (**P-Q**) Representative immunoblots (**P**) and quantitative results (**Q**) of indicated proteins in WT cells expressing control gRNA (Ctrl gRNA) or gRNAs targeting STAT3 (STAT3 gRNA) upon exposure with or without IFNγ for 16 hours. (**R**) Immunoblot of c-Myc in control and c-Myc overexpressing KO cell lines. Data are representative of at least two independent experiments with similar results. Data are means ± s.e.m. and analyzed by two-tailed, paired (A, B, D)] or unpaired (G, I, K, M, O, and Q) Student's t-test.

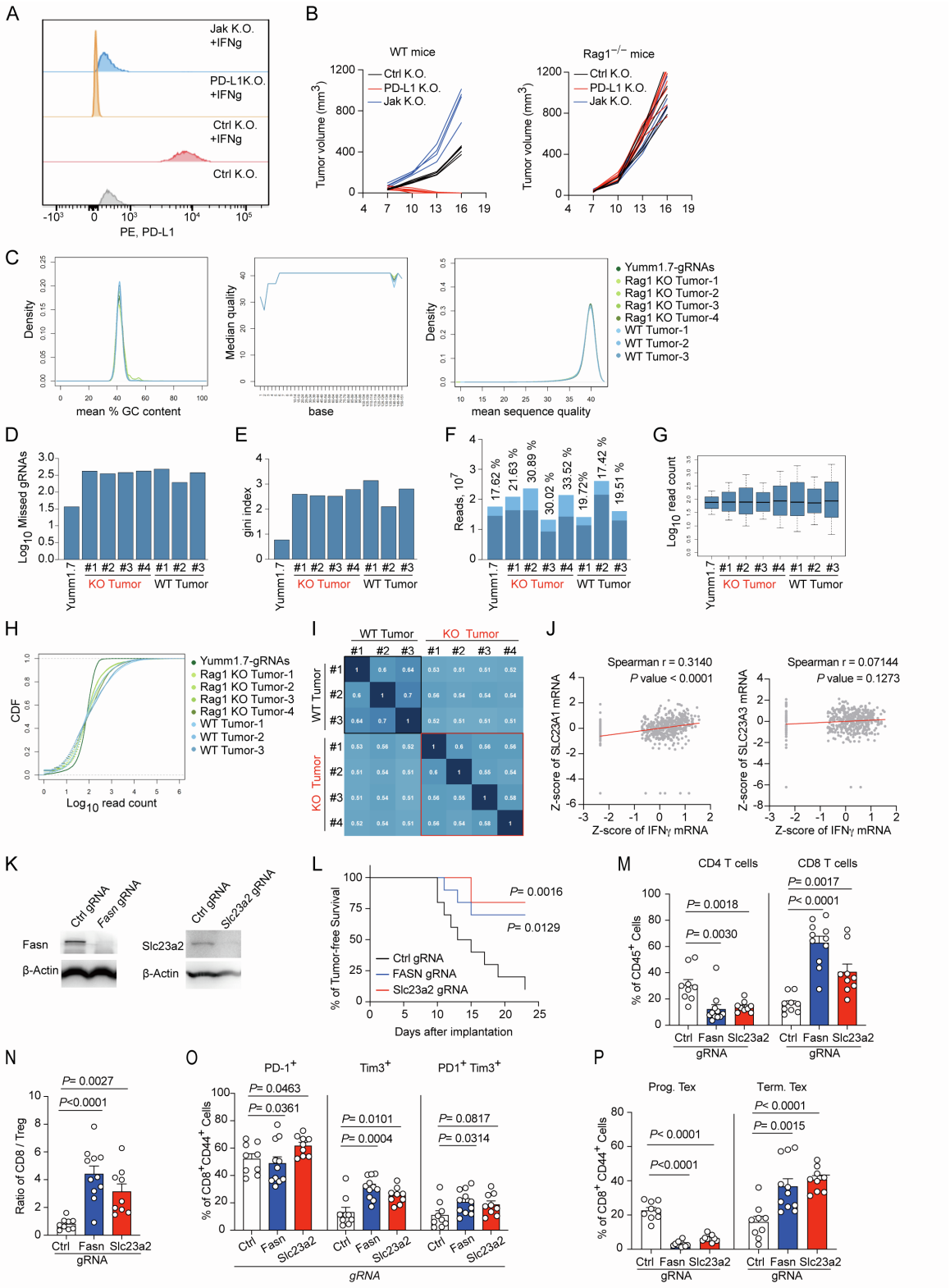


**Figure S6. Analysis of screen performance and validation data for screen hits, Related to Figure 6.**

(**A**) Histogram of the geometric MFI of PD-L1 surface staining in Yumm1.7 cas9 cell with indicated treatment. (**B**) Tumor growth of Yumm1.7 tumors treated with indicated gRNAs in WT (B6 Cas9; left) mice and Rag1$^{-/-}$ mice (right), n=5-7 mice per group). (**C** to **I**) The quality control (QC) view of MAGeCK-VISPR for Yumm1.7 cells and indicated tumor samples, include the distribution of GC

content (C, left), median base quality (C, middle), the distribution of mean sequence quality (C, right), the number of zero-count sgRNAs (D), Gini-index (E), total number of reads and the percentage of mapped reads (F), normalized read count distribution (G and H), and pairwise sample correlations (I). **(J)** Spearman correlation analysis for Z-score of slc23a1 (left) or slc23a3 (right) expression with IFNγ (n = 401 biologically independent melanoma tumor samples from TCGA cohort). (**K**) Immunoblot of Fasn and Slc23a1 in control, Fasn-null or Slc23a2-null Yumm1.7 cells. (**L)** Tumor-free survival curves of B16 melanomas were determined as indicated (n = 10 per group). **(M**) Quantification of $CD4^+$ and $CD8^+$ cell populations among $CD45^+$ TILs isolated from the YUMM1.7 melanomas with similar size (Ctrl gRNA: n = 9; *Fasn* gRNA: n = 11; *Slc23a2* gRNA: n = 9). (**N**) Ratio of $CD8^+$ versus Treg after quantifying the percentage of $CD8^+$ T cells and $FOXP3^+$ Treg cells among $CD45^+$ cells (Ctrl gRNA: n = 9; *Fasn* gRNA: n = 11; *Slc23a2* gRNA: n = 9). (**O**) Exhausted T cell populations, including PD-$1^+$, $Tim3^+$, and PD-$1^+Tim3^+$, were quantified among activated $CD8^+$ TILs isolated from YUMM1.7-SCAR tumors with similar size (Ctrl gRNA: n = 9; *Fasn* gRNA: n = 11; *Slc23a2* gRNA: n = 9). (**P**) Quantification of progenitor and terminally exhausted T cell population among activated $CD8^+$ TILs, which were determined by PD-$1^+TCF1^+Tim3^-$ and PD-$1^+TCF1^-Tim3^+$, respectively (Ctrl gRNA: n = 9; *Fasn* gRNA: n = 11; *Slc23a2* gRNA: n = 9). Data are representative of two independent experiments with similar results (A, B, and L-P). Data are analyzed by two-tailed, paired (M-P) or Log-rank test (L).